Spatial solitons in quadratic 2D nonlinear photonic crystals

Katia Gallo, Alessia Pasquazi,* Salvatore Stivala,* Gaetano Assanto*
Optoelectronics Research Centre, University of Southampton, SO17 1BJ, United Kingdom
** NooEL, via della Vasca Navale 84, University "Roma Tre", 00146 Rome, Italy*
Tel: +44 23 8059 7673, Fax: +44 23 8059 3149, e-mail: kag@orc.soton.ac.uk

ABSTRACT
We report on the first investigations into parametric solitary-wave formation in 2D nonlinear photonic crystals and present experimental results obtained in an hexagonally poled $LiNbO_3$ waveguide designed for twin-beam second harmonic generation at telecom wavelengths.
Keywords: nonlinear optics, photonic crystals, spatial solitons, waveguides, lithium niobate.

1. INTRODUCTION

Self-guiding filaments of light or optical spatial solitons, resulting from the balance between nonlinearity and diffraction, hold promise for the development of novel, reconfigurable photonic architectures for switching and routing. They have been predicted and demonstrated in a variety of physical settings [1], including quadratic media. In the latter case, diffractive beam spreading is counteracted by the parametric interplay of three wavelength components, resulting in the mutual trapping and locking of multi-frequency waves (i. e. multicolour solitons). The original predictions on soliton formation via three-wave mixing [2] were confirmed nearly a decade ago by the first experiments carried out in KTP and $LiNbO_3$ [3-4]. Since then, the development of Quasi-Phase-Matching (QPM) materials such as Periodically Poled $LiNbO_3$ (PPLN) has opened up new possibilities for quadratic soliton science and engineering [5-6].QPM has also recently been extended to higher-dimensionalities, to demonstrate 2D PPLN Nonlinear Photonic Crystals (NPC), i.e. 2D lattices in the second-order susceptibility $\chi^{(2)}$, enabling novel and more versatile geometries for parametric interactions [7-8].

Here we report the first experimental and theoretical investigations on soliton formation in two-dimensional NPCs, using hexagonal lattices in lithium niobate. The study was performed in a (1+1)D configuration, using buried planar waveguides embedded in the NPC structure for maximum efficiency [9]. The results unveil an excitingly rich scenario for soliton physics and optical processing, arising as a result of multiple spatial - as well as spectral - nonlinear resonances in the 2D nonlinear lattice.

2. THE QPM CONFIGURATION

The structure of the two-dimensional NPC used for the experiments is schematically shown in Fig.1*a*. An hexagonal modulation of the nonlinear susceptibility $\chi^{(2)}$ (period Λ=16.4 μm) in the X-Y crystal plane (Fig. 1*b*) translates into the availability of multiple reciprocal lattice vectors for QPM (Fig. 1*c,* Fourier plane). In particular, our HexLN (Hexagonally poled $LiNbO_3$) lattice was designed to allow efficient twin-beam second harmonic generation (SHG) from $\lambda_\omega \sim 1.55$ μm, involving the fundamental order (TM_0) modes of a high-efficiency planar waveguide embedded in the crystal [9].

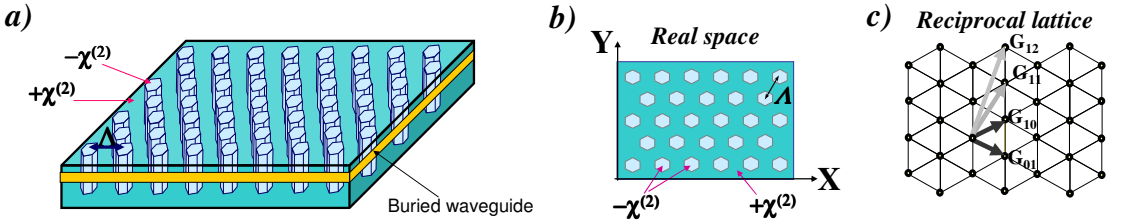

Figure 1. a) *Sketch of the 2D NPC waveguide enabling twin-beam second harmonic generation;* ***b)*** *its 2D* $\chi^{(2)}$ *modulation in real space (X-Y plane of* $LiNbO_3$*);* ***c)*** *the lattice in Fourier space (*$\mathbf{G}_{mn}$*=reciprocal lattice vectors).*

The 2D QPM configuration used for twin-beam SHG in the nonlinear lattice is illustrated in Fig.2. A fundamental beam (ω) propagating along the X axis (Fig. 2*a*: symmetric case), or at a small angle (θ_ω) with respect to it (Fig. 2*b*: asymmetric case), excites two SHG resonances, on either side, quasi-phase-matched by two low-order reciprocal lattice vectors ($\mathbf{G}_{10}$ and $\mathbf{G}_{01}$, respectively). The twin-beam QPM configuration allows SHG

K.G's work was funded by the Leverhulme Trust through a Special Research Fellowship (SRF/40112). The authors in NooEL acknowledge partial support from MIUR (National Project nr. 2005098337).

tuning from degeneracy for coincident resonances: $\lambda_1=\lambda_2=\lambda_0$ (fig. 2*a*) to fully decoupled SHG processes $\lambda_1\neq\lambda_2$ (fig. 2*b*) through adjustments in the propagation angle of the fundamental beam in the crystal (fig. 2*c*).

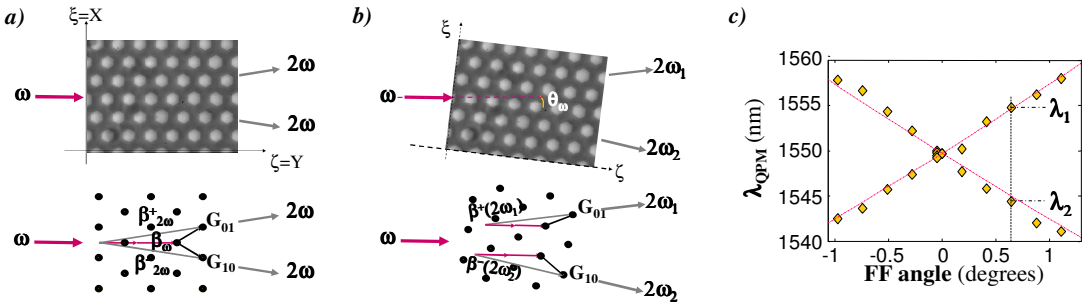

Figure 2. *QPM configuration for twin-beam SHG in the HexLN waveguide.* ***a)*** *symmetric ($\theta_\omega=0$);* ***b)*** *asymmetric ($\theta_\omega\neq0$) SHG.* ***c)*** *tuning of the two SHG resonances with the fundamental (FF) incidence angle.*

3. THE MODEL

With reference to the direction ζ along which the pump (FF) beam is launched and an orthogonal axis ξ (i.e. $\boldsymbol{\zeta}=\boldsymbol{\beta}_\omega/|\boldsymbol{\beta}_\omega|$; $\boldsymbol{\zeta}\perp\boldsymbol{\xi}$), the twin-beam SHG process can be modeled through the following coupled-mode equations:

$$\begin{aligned}
&\frac{\partial A}{\partial\zeta}+i\sigma\frac{\partial^2 A}{\partial\xi^2}=-i\Gamma^{+}\,A^{*}B^{+}-i\Gamma^{-}A^{*}B^{+}\\
&\frac{\partial B^{+}}{\partial\zeta}+\rho^{+}\frac{\partial B^{+}}{\partial\xi}+i\sigma^{+}\frac{\partial^2 B^{+}}{\partial\xi^2}+i\,\delta\beta^{+}\,B^{+}=-i\Gamma^{+}A^{2}\\
&\frac{\partial B^{-}}{\partial\zeta}+\rho^{-}\frac{\partial B^{-}}{\partial\xi}+i\sigma^{-}\frac{\partial^2 B^{-}}{\partial\xi^2}+i\,\delta\beta^{-}\,B^{-}=-i\Gamma^{-}A^{2}
\end{aligned}\qquad(1)$$

where A and $B^{\pm}$ are the slowly-varying envelopes of the FF and SH waves. $\zeta=x/L_D$ and $\xi = y/w_0$ are the longitudinal and the transverse coordinates, normalized to the FF diffraction length ($L_D=\beta_\omega w_o^2/2$) and the input beam waist (w_0), respectively. Equations (1) account for diffraction at the FF and at the SH ($\sigma = 1/4$ and $\sigma^{\pm}\sim 1/8$, respectively), as well as for in-plane angular deviations of the SH beams due to noncollinear QPM ($\rho^{\pm}\sim\pm 1.5$). The two SHG processes are characterized by normalized coupling coefficients: $\Gamma^{\pm}$ and mismatches: $\delta\beta^{+} = [\beta_{2\omega}{}^{+} -2\beta_\omega- G_{01}]\,L_D$ and $\delta\beta^{-} = [\beta_{2\omega}{}^{-} -2\beta_\omega- G_{10}]\,L_D$. As $\Gamma^{+}\cong\Gamma^{-}$, the nonlinear wave dynamics is essentially determined by the interplay between $\delta\beta^{+}$ and $\delta\beta^{-}$. Maps such as the ones shown in Fig. 3, obtained by solving equations (1) with a split-step beam propagation algorithm, can be used to analyse the effect of the SHG parameters on the FF response, here characterised in terms of the width (Fig. 3*a*) and the lateral shift (fig. 3*b*) of the FF emerging from the 2D NPC. From the simulation results it is apparent that the additional degrees of freedom associated to the double resonance can yield substantially different results from the 1D SHG soliton regime, with an enhanced range for FF wave confinement (regions of $\delta\beta\sim 0^{+}$, Fig. 3*a*) and opposite beam displacements with respect to the input direction (Fig. 3*b*).

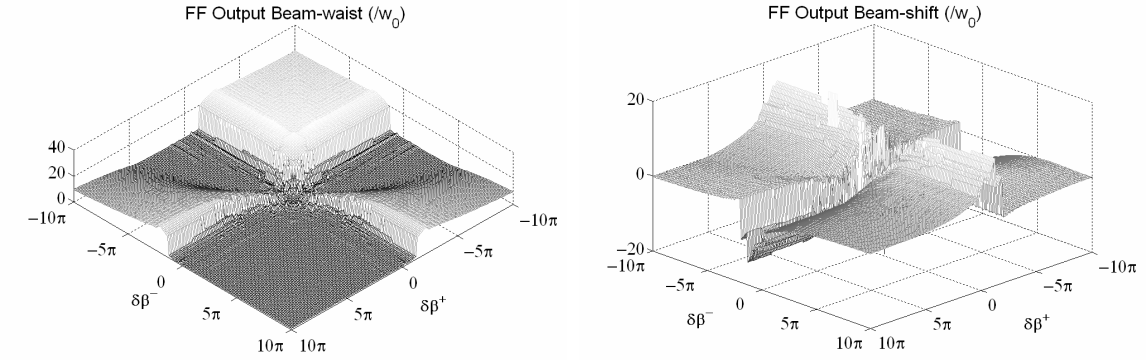

Figure 3. *Contour plots showing the output FF beam lateral width and displacement (in units of w_0) as a function of the two SHG phase-mismatches ($\delta\beta^{+}$ and $\delta\beta^{-}$).*

4. THE EXPERIMENTS

For the nonlinear optical experiments, the HexLN waveguide was mounted on a piezo-electrically controlled stage and kept at ~ 85°C to prevent photorefractive damage. The FF propagation angle (θ_ω) was adjusted by rotating the crystal. We pumped the HexLN waveguide at wavelengths in the 1.1–1.6 μm range, with narrow line-width (< 0.2 cm^{-1}) 20 ps pulses delivered by an optical parametric generator operating at 10 Hz. The FF input Gaussian transverse profile (TEM_{00}) was shaped into a cylindrical spot (lateral and vertical beam waists: w_0=27.5 μm and v_0=3.4 μm, respectively) and end-fire coupled to excite the TM_0 mode of the planar waveguide. Its propagation in the HexLN device (18 mm-long) amounted to ~5.4 diffraction lengths (L_D). The FF (SH) energies and lateral beam profiles were monitored with time-gated photodiodes, or imaged on a Vidicon (Si-CCD) camera. The experimental setup is schematically shown in Fig. 4.

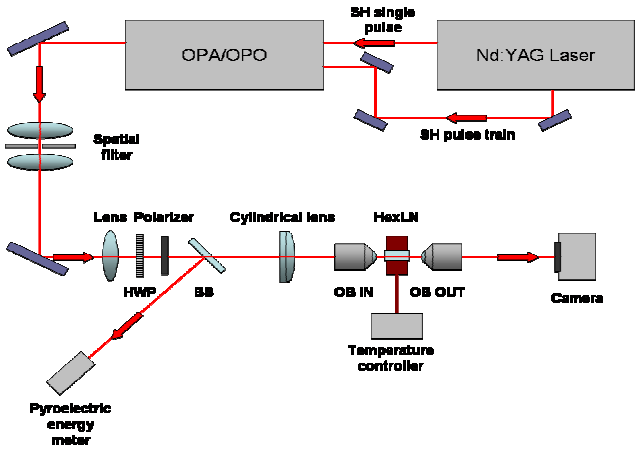

Figure 4. Setup for soliton experiments in the 2D nonlinear photonic crystal (HexLN) waveguide.

For a quantitative study of self-confinement associated to twin-beam SHG, we systematically monitored the evolution of the FF response, i.e. spot-size and lateral displacement at the output, as a function of the main control parameters, i.e.: input wavelength (λ_ω), launch peak-power (P_ω) and angle of propagation (θ_ω) of the FF pump. In the model of equations (1), P_ω affects the coupling coefficients ($\Gamma^{\pm} \propto \sqrt{P_\omega}$), while λ_ω and θ_ω determine the values of the mismatches [through the empirical formula: $\delta\beta^{(\pm)} = -0.51\pi\,(\lambda_\omega - \lambda_0)|_{nm} \pm 4.06\pi\cdot\theta_\omega|_{deg}$].

In the experiments we could observe an extremely rich wave dynamics. In general, for pump wavelengths close to the SHG resonances, i.e. $\lambda_\omega = \lambda_1 + \delta\lambda$ or $\lambda_\omega = \lambda_2 + \delta\lambda$, with $\delta\lambda > 0$, we could observe FF self-confinement to lateral widths comparable to the input for $P_\omega \geq 20$kW.

The soliton response to increasing pumping levels (external peak powers) is presented in Figure 5. The plot in Fig. 5*a* shows experimental results obtained close to degeneracy, while those in Fig. 5*b-c* refer to the case of spectrally distinct SHG resonances, i.e. asymmetric twin-beam SHG ($\theta_\omega = 0.54^o$), at $\lambda_\omega = \lambda_1 + \delta\lambda$ (Fig.5*b*) and $\lambda_\omega = \lambda_2 + \delta\lambda$ (Fig.5*c*). In the symmetric configuration, corresponding to frequency-degenerate SHG ($\lambda_1 = \lambda_2 = \lambda_0$ and $\delta\beta^+ = \delta\beta^-$), the FF beam progressively narrows as P_ω increases, becoming double-humped in the interval $30 < P_\omega < 60$ kW (see insets above Fig. 5*a*). The appearance of two peaks matches the predictions from equations (1) and suggests the formation of compound soliton states. In the non-symmetric case, the FF beam progressively narrows until saturation is reached, while still remaining single-humped throughout the explored power range. At the same time, it is displaced in the transverse direction, towards either positive or negative values of ξ (cf Fig. 2), depending on the predominant "pulling" action of either SH beam. Hence the trend towards a negative shift in Fig. 5*b* (when $\lambda_\omega \sim \lambda_1$, with $\delta\beta^- \sim 0^+$) and the positive displacement observed in Fig. 5*c* (when $\lambda_\omega \sim \lambda_2$, with $\delta\beta^+ \sim 0^+$).

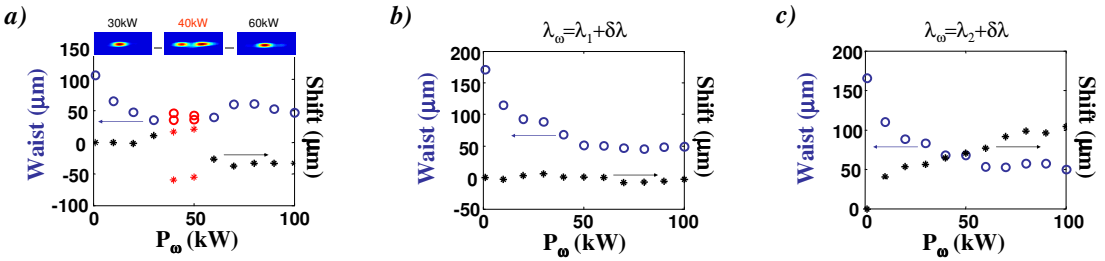

Figure 5. *FF power response for:* ***a)*** $\theta_\omega \sim 0^o$, $\lambda_\omega \sim \lambda_0 + 1.5$ nm, $\theta_\omega \sim 0.54^o$: ***b)*** $\lambda_\omega \sim \lambda_1 + 1.5$ nm; ***b)*** $\lambda_\omega \sim \lambda_2 + 0.5$ nm

The effect of the input wavelength in the solitonic regime is illustrated by Figure 6. For symmetric SHG (Fig. 6*a*) we could observe an enhanced spectral range for FF beam confinement (almost twice the range for conventional 1D SHG). As the "pulling" actions of the two SH beams tend to balance each other, the FF tends to maintain its original direction of propagation (i.e. FF shift ~0). On the other hand, when the two SHG resonances are brought apart (by increasing $|\theta_\omega|$), two distinct spectral regions for FF confinement appear in the response, each of them corresponding to opposite displacements, as seen in Fig. 6*b*. This entails light routing by acting on the input wavelength (λ_ω), an entirely new approach to soliton steering, not possible for conventional, single-resonance SHG solitons.

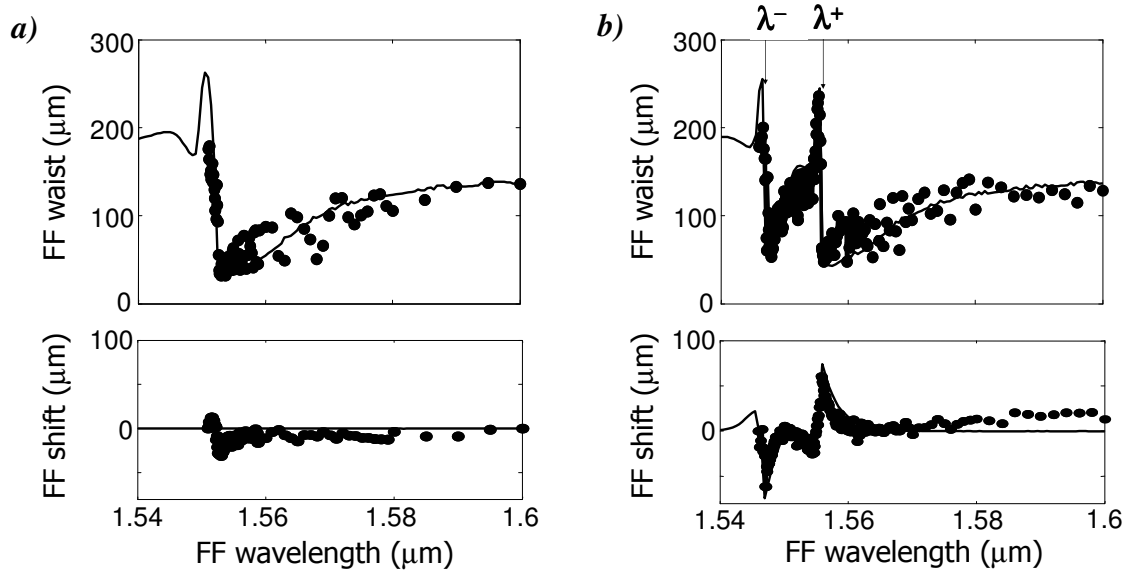

Figure 6. *FF beam waist and lateral shift measured at the 2D NPC output (dots) as a function of the input wavelength for* ***a)*** $\theta_\omega \sim 0^o$, $P_\omega = 25$ kW *and* ***b)*** $\theta_\omega \sim 0.58^o$, $P_\omega = 22$ kW. *The solid lines are predictions from eq. 1.*

5. CONCLUSIONS

In conclusion, we have presented the first results on a novel class of parametric solitary waves, sustained by multiple quadratic resonances in a 2D nonlinear photonic crystal. By implementing a twin-beam SHG configuration in a HexLN planar waveguide we demonstrated the existence of two spectral regions for beam confinement and opposite displacements controllable with the input FF wavelength, angle and power. These findings open up an exciting new scenario in the field of quadratic solitons, paving the way towards multicolor solitary wave engineering with higher dimensionality nonlinear photonic crystals, aperiodic lattices and quasi-crystals in ferroelectric materials.

REFERENCES

[1] Y. S. Kivshar and G. P. Agrawal, *Optical Solitons: from fibres to photonic crystals*, Academic, New York, 2003.

[2] Y. N. Karamzin and A. P. Sukhorukov, Mutual focusing of high-power light beams in media with quadratic nonlinearity, *Sov. Phys. JETP, vol. 41, pp. 414-420, 1976.*

[3] W. E. Torruellas *et al.*, Observation of two-dimensional spatial solitary waves in a quadratic medium, *Phys. Rev. Lett., vol. 74, pp. 5036-5039, 1995.*

[4] R. Schiek, Y. Baek, G. I. Stegeman, One-dimensional spatial solitary waves due to cascaded second-order nonlinearities in planar waveguides, *Phys. Rev. E, vol. 53, pp. 1138-1141, 1996.*

[5] B. Bourliaguet *et al.*, Observation of quadratic spatial solitons in periodically poled lithium niobate, *Opt. Lett. vol. 24, pp. 1410-1412, 1999.*

[6] R. Schiek *et al.*, One-dimensional spatial soliton families in optimally engineered quasi-phase-matched lithium niobate waveguides, *Opt. Lett. vol. 29, pp. 596-598, 2004.*

[7] V. Berger, Nonlinear Photonic Crystals, *Phys. Rev. Lett., vol. 81, pp. 4136-4139, 1998.*

[8] N. G. R. Broderick, G. W. Ross, H. L. Offerhaus, D. J. Richardson, D. C. Hanna, Hexagonally poled lithium niobate: a two-dimensional nonlinear photonic crystal, *Phys. Rev. Lett., vol. 84, pp. 4345-4348, 2000.*

[9] K. Gallo *et al.*, Guided-wave second harmonic generation in a $LiNbO_3$ nonlinear photonic crystal, *Opt. Lett. vol. 31, pp. 1232-1234, 2006.*